

Stereotactic Body Radiotherapy for Lung Lesions using Multiple Phase 3D-CT Based on the Analysis of Radiobiological Parameters

Arun Chairmadurai^{1*}, Harish Chandra Goel², Sandeep Kumar Jain¹, Pawan Kumar¹

1. Department of Radiation Oncology, Jaypee Hospital, Noida, India

2. Amity Centre for Radiation Biology, Amity University, Noida, India

ARTICLE INFO	ABSTRACT
<p>Article type: Original Article</p> <p>Article history: Received: Sep24, 2018 Accepted: Dec01, 2018</p> <p>Keywords: SBRT-Lung Radiobiology Volumetric-Modulated Arc Therapy</p>	<p>Introduction: Planning target volume (PTV) is generated from internal treatment volume (ITV) using four-dimensional computed tomography (4D-CT) for enhanced therapeutic gain in the stereotactic body radiotherapy for lung lesions (SBRT-Lung). This study aimed to propose a strategy to generate ITV on multiple-phase 3D-CT and enhance therapeutic gain in SBRT-Lung.</p> <p>Material and Methods: This study was conducted on 6 peripherally located and 5 centrally located lung lesions suitable for SBRT. The PTV was delineated based on 3D-CT datasets acquired at three different phases of respiratory motion. The prescribed dose of 50 Gy in 5 fractions was delivered using RapidArc technique. The therapeutic-gain was compared based on tumor control probability (TCP) and normal tissue complication probability (NTCP) against a multicenter trial, which uses single-phase 3D-CT for PTV delineation. The TCP and NTCP were calculated by Poisson's linear-quadratic and Lyman-Kutcher-Burman models, respectively.</p> <p>Results: Regarding the multicentre trial, the PTVs were maximally reduced to 42% and 57% among the 6 peripherally and 5 centrally located lung lesions, respectively. In peripheral lung lesions, TCP was significantly enhanced to 0.6% for long-term (>5years) local control ($P<0.05$), and NTCP was significantly reduced in pneumonitis (Grade\geqII) of lung (0.2%; $P<0.05$). In central lung lesions, TCP was insignificantly enhanced; however, NTCPs were maximally reduced for cartilage necrosis in trachea (35%) and myelitis in spinal cord (19%).</p> <p>Conclusion: The proposed strategy reduced the complications for normal tissues and enhanced therapeutic gain. The successful clinical outcomes validated our hypothesis in short-term (6-12 months), and we are currently testing the long-term efficacy.</p>

► Please cite this article as:

Chairmadurai A, Chandra Goel H, Kumar Jain S, Kumar P. Stereotactic Body Radiotherapy for Lung Lesions using Multiple Phase 3D-CT Based on the Analysis of Radiobiological Parameters. Iran J Med Phys 2019; 16:270-279.10.22038/ijmp.2018.35064.1438.

Introduction

Stereotactic body radiotherapy (SBRT) delivers an ablative radiation dose to tumors that are located at inoperable sites and are closely aligned with normal organs. The SBRT can lead to the non-invasive achievement of the high rates of local control for lung lesions (up to 90%); therefore, SBRT is widely considered an effective alternative to lobectomy for early-stage non-small cell lung cancer (stage I) [1-4]. Advanced technologies used for radiotherapy reduce toxicity to normal tissue and enhance the quality of post-treatment life [5-7]. The efficiency of SBRT in delivering an ablative dose to the tumor relies on the generation of a robust planning target volume (PTV) from the gross tumor volume (GTV) using three-dimensional computed tomography (3D-CT) images.

Respiratory motion is a major challenge for the delineation of a robust PTV in lung-SBRT. Internal treatment volume (ITV) is the volume within which

the tumor oscillates during a particular breathing pattern. The ITV is generated by combining GTV and internal margin (IM). The IM is the margin for drift of tumor during respiratory motion [8]. The IM has been derived by different tumor tracking systems, such as fluoroscopy, orthogonal portal image, dynamic magnetic resonance image, multiple-phase 3D-CT, and four-dimensional computed tomography (4D-CT). During respiratory motion, the lung lesion oscillates more in craniocaudal direction than in transversal direction [9-14]. The PTV has been widely delineated either by 4D-CT or 3D-CT protocol in a multicenter trial for lung-SBRT [15]. The trial recommends the delineation of PTV either by expanding ITV with 5-mm isotropic margin on 4D-CT [16] or expanding the GTV with 5-mm margin in the axial direction and 10-mm margin in the longitudinal direction on 3D-CT [3].

The delineation of PTV margins from ITV is more robust and reproducible in lung-SBRT. As a result, PTVs are preferably delineated with the 4D-CT protocol than 3D-CT protocol in multicenter trials. The delineation of PTV for lung-SBRT by expanding GTV with additional margins on 3D-CT yields larger treatment volume up to two times more than expanding ITV with additional margins either on 4D-CT or multiple-phase 3D-CT [17-20]. Subsequently, this study was motivated to propose a strategy to delineate PTVs from ITVs on multiple-phase 3D-CT for lung-SBRT. The evaluation of tumor response to a treatment regimen is based on 'Response Evaluation Criteria in Solid Tumors' (RECIST) [21].

The clinical outcome depends on various prognostic factors in tandem to SBRT-Lung. The analyses of radiobiological parameters reveal the quality of radiotherapy delivered through different PTV delineation protocols for lung-SBRT. Tumor control probability (TCP) and normal tissue complication probability (NTCP) are the two radiobiological parameters available for evaluating the efficiency of PTV delineation protocols. Various radiobiological models of cell survival curves have been used for a high-dose-hypo-fractionated scheme of SBRT [22-27]. Poisson's linear-quadratic (PLQ) cell survival model has been used in conventional 2-Gy/fraction dose regimens (EQD₂) and recent studies have supported their applicability in estimating the TCP for SBRT-Lung [28-30].

In the current study, PLQ and Lyman-Kutcher-Burman (LKB) models were employed to calculate the relative efficiencies of different radiotherapy plans. The purpose of this study was to investigate the impact of PTV delineation based on radiobiological parameters in peripherally and centrally located lung lesions for SBRT-Lung patients. The researchers hypothetically tested the radiobiological parameters for radio-therapeutic gain with a change in PTV delineation strategies. This comparative study reported (i) multiple-phase 3D dose calculation in order to account the respiratory motion and observed variations in radiobiological parameters, (ii) normal tissue complications due to a generous planning target volume, and (iii) post-treatment set-up errors in terms of observed variations in radiobiological parameters.

Materials and Methods

Treatment Simulation and Target Delineation

This study was conducted on 6 peripherally located and 5 centrally located lung lesions suitable for SBRT (Table1). 7 patients were immobilized on a Vac-Lok cushion with indexing features (M/s.Civco, Coralville, IA, USA) using a pneumatic abdominal compression system, as described by Lovelock et al. [31]. The pneumatic abdominal compression system used in this study consisted of a commercially available sphygmomanometer (M/s. WelchAllyn®, Skaneateles Falls, NY, USA) and nylon strap with a Velcro™ fastener. The CT datasets were acquired using a helical CT machine (Biograph; M/s. Siemens Healthcare, Erlangen, Germany).

Lesions located within 2-cm from the proximal bronchial tree are considered as centrally located and others are categorized as peripherally located lung lesions.

Patients were trained to perform shallow breathing, and baseline CT datasets for planning purposes were acquired at random breathing phase. More CT datasets with deep inspiration breath-hold (DIBH) and deep expiration breath-hold (DEBH) phases were acquired for evaluating IMs. The strategy was approved by the Ethics Committee of the Cancer Care of Jaypee Hospital, Noida, India. Baseline CT datasets were considered for GTV delineation. The IMs for accommodating the movements of GTV during respiratory motions were taken from CT datasets acquired at DIBH and DEBH, by which ITV was subsequently delineated. The ITV was further expanded with 3-mm margin to generate the PTV on baseline CT datasets. Critical organs, such as the lungs, ribs, esophagus, trachea, spinal cord, and heart, were also contoured on the baseline CT datasets.

Treatment Planning

The SBRT-Lung was delivered on TrueBeamSTx platform Linac (Varian Medical Systems, Palo Alto, CA) equipped with HD120™ MLC. Treatments were planned using the Eclipse External Beam Planning (Version 13.0.33). The prescription dose to PTV was 50 Gy delivered in 5 fractions using RapidArc technique. The RapidArc plan consisted of 2 co-planar treatment arcs (first in a clockwise direction - 181° to 179° and second in a counter-clockwise direction - 179° to 181°).

Table1. Summary of distribution of lung lesions in patients

Patient No.	Histology	Tumor Stage	No. of Lesions	Location	
				Peripheral	Central
1	Intraductal Carcinoma	IV	1	1	-
2	Squamous Cell Carcinoma	IIB	1	-	1
3	Hepatocellular Carcinoma	IV	2	1	1
4	Squamous Cell Carcinoma	IA	1	-	1
5	Squamous Cell Carcinoma	IVB	1	1	-
6	Adenocarcinoma	IVA	2	2	-
7	Adenocarcinoma	IVA	3	1	2
Total			11	6	5

Table 2. Summary of radiobiological cost functions for the calculations of tumor control probability and normal tissue complication probability

Structure	Endpoint/Stage	Biological Model	D ₅₀ (Gy)	α/β (Gy)	γ	s	n	m
GTV & ITV	36-month local control	PLQ	42.3	10	0.9	-	-	-
	Long term (> 5 years) local control	PLQ	49.2	10	1	-	-	-
Lung	Pneumonitis, Grade - \geq II	LKB	30.8	3	-	-	0.99	0.37
Rib	Pathologic fracture	PLQ	65.0	3	2.3	1	-	-
Esophagus	Esophagitis, Grade - \geq II	LKB	51.0	10	-	-	0.44	0.32
Trachea	Cartilage necrosis	PLQ	78.8	3	4.8	0.66	-	-
Spinal Cord	Necrotic Myelitis	PLQ	68.6	3	1.9	4	-	-
Heart	Pericarditis	PLQ	49.2	3	3	0.2	-	-

GTV: gross tumor volume, ITV: internal target volume, PLQ: Poisson linear-quadratic model [35-37], LKB: Lyman-Kutcher-Burman model [38-39], D₅₀: rate of control and complication at 50% for TCP and NTCP, respectively, α/β : dose at which linear and quadratic components of cell killing are equal, γ : normalized dose-response gradient at maximum, s: parameter to account relative seriality of an organ's internal organization, m: slope of the cell survival curve, n: parameter to account irradiated volume of an organ

Progressive resolution optimizer (Version 13.0.26) was utilized for RapidArc optimization, and the jaws were set for tracking PTV by enabling the "Jaw Tracking" option. Acuros External Beam (Version 13.0.26) was employed to compute volumetric doses to heterogeneous medium with 1-mm grid resolution [32]. Patient's treatment set-up was verified by On-Board Imager® (OBI) and accurately repositioned on PerfectPitch™ couch with 6 degrees of freedom. Patients were reminded to perform shallow breathing during image verification and treatment. Target localization and set-up verification before and after treatment were accomplished based on cone-beam computed-tomography acquired by OBI and baseline CT datasets. The target localization and set-up verification procedures for SBRT-Lung were performed as described by other medical professionals [33,34].

Comparison with Multicenter Trial

The PTV delineation protocols of radiation therapy oncology groups (RTOG) multicenter trial- 0915 [15] was considered to evaluate the efficiency of the proposed strategy to delineate PTV using multiple-phase 3D-CT in SBRT-Lung. The protocol [15] for PTV delineation in SBRT-Lung (i.e., GTV with an additional margin of 5-mm in transversal and 10-mm in longitudinal planes from single-phase 3D-CT) was used to generate standard PTV (PTV2), which was compared with the efficiency of the proposed PTV (PTV1) delineated with multiple-phase 3D-CT strategy. Consort diagram for this comparison study is displayed in Figure 1. The original plan delivered to the patient was considered as the proposed plan (PP). The RapidArc with identical beam arrangement was planned retrospectively to deliver the prescribed dose to standard PTV (PTV2) and renormalized identically to mean dose received by ITV in PP. The results of the obtained plan were considered the standard plan (SP) and was compared with the PP.

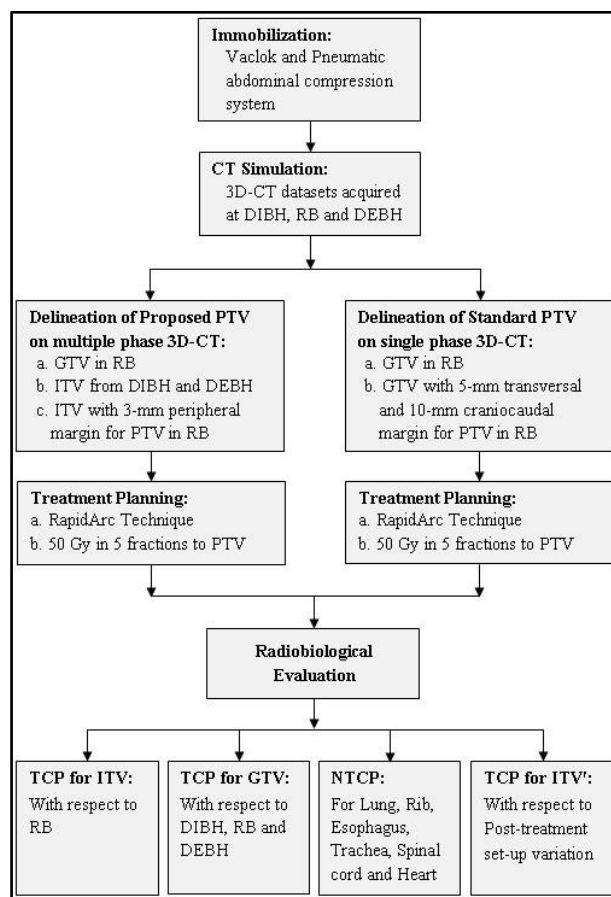


Figure 1. Consort diagram for the comparative study of strategies used for delineating planning target volumes from 3D-CT and comparing radiobiological parameters during respiratory movements and post-treatment set-up variations

Radiobiological Analysis

Radiobiological parameters, such as TCP and NTCP, were evaluated based on the dose-volume histogram of both the SBRT-Lung plans (PP and SP). Radiobiological estimates were evaluated in Biological Evaluation software (M/s. Varian Medical Systems) using PLQ and LKB models. The PLQ model was based on cell survival model with Poisson distribution, whereas the LKB model was based on cell survival model with a standard normal distribution. Table2

tabulates the cost functions of cell survival model used for the evaluation of TCP and NTCP [32, 35-39]. The radiobiological parameters of the both plans were evaluated in the aspects of tumor displacement and tissue heterogeneity during the respiratory movements and reproducibility of dose delivery beyond treatment set-up variations. The effectiveness of PTV delineation protocols was analyzed for the enhancement of TCP and reduction of NTCP using two-tailed paired sample t-test. The difference between PP and SP was considered significant ($P < 0.05$).

Results

The GTVs, the resultant ITVs, and PTVs were within the range of 2-22 cm³ (Table3). Internal margins for ITV due to respiratory movements of GTV varied with respect to tumor size and location (Table3). The

IMs were found negligible for centrally located lung lesions but enlarged to more than 120% of the GTV for peripherally located lung lesions. The proposed PTV was found smaller than the standard PTV up to 42-57% in peripherally and centrally located lung lesions, respectively. As the standard PTVs were delineated solely from GTV, it was independent of ITV. Consequently, the inclusion of ITV in standard PTV varied from 100% to 79% in peripherally located lung lesions. Due to negligible IMs in each centrally located lung lesion, 100% of ITVs were included in the entire standard PTVs. This variation in the inclusion of ITVs within proposed and standard PTVs altered the dose distribution in ITV (Figure 2). As a result, the tumor control probability varied with dose distribution in the treatment target at different breathing phases (Table4).

Table 3. Characteristics of treatment volumes in peripherally and centrally located lesions

S.No.	GTV (cm ³)	ITV (cm ³)	PTV1 (cm ³)	PTV2 (cm ³)	ITV∩PTV2 (cm ³)	Enlargement of Internal Margins (%)	Reduction of PTV (%)	Inclusion of ITV within PTV2 (%)
Peripherally Located Lesions								
1	1.60	2.50	6.50	11.30	2.20	56.25	42.48	88.00
2	2.40	4.70	11.70	15.40	3.70	95.83	24.03	78.72
3	3.00	4.50	10.50	16.90	4.50	50.00	37.87	100.00
4	3.20	5.00	12.00	19.30	5.00	56.25	37.82	100.00
5	5.20	11.60	24.70	24.30	11.30	123.08	-1.65	97.41
6	11.20	17.40	34.10	43.60	17.00	55.36	21.79	97.70
Mean	4.43±3.22	7.62±5.21	16.58±9.63	21.80±10.51	7.28±5.20	72.79±27.17	27.06±14.90	93.64±7.81
Centrally Located Lesions								
1	2.30	2.30	8.50	16.80	2.30	0.00	49.40	100.00
2	2.40	2.40	6.90	16.00	2.40	0.00	56.88	100.00
3	4.30	4.30	13.40	24.10	4.30	0.00	44.40	100.00
4	5.50	5.50	13.00	28.60	5.50	0.00	54.55	100.00
5	22.20	22.20	38.60	63.10	22.20	0.00	38.83	100.00
Mean	7.34±7.53	7.34±7.53	16.08±11.54	29.72±17.33	7.34±7.53	0.00±0.00	48.81±6.59	100.00±0.00

GTV: gross tumor volume, ITV: internal treatment volume, PTV1: proposed planning target volume, PTV2: standard planning target volume, ITV∩PTV2 – ITV intersecting with standard PTV

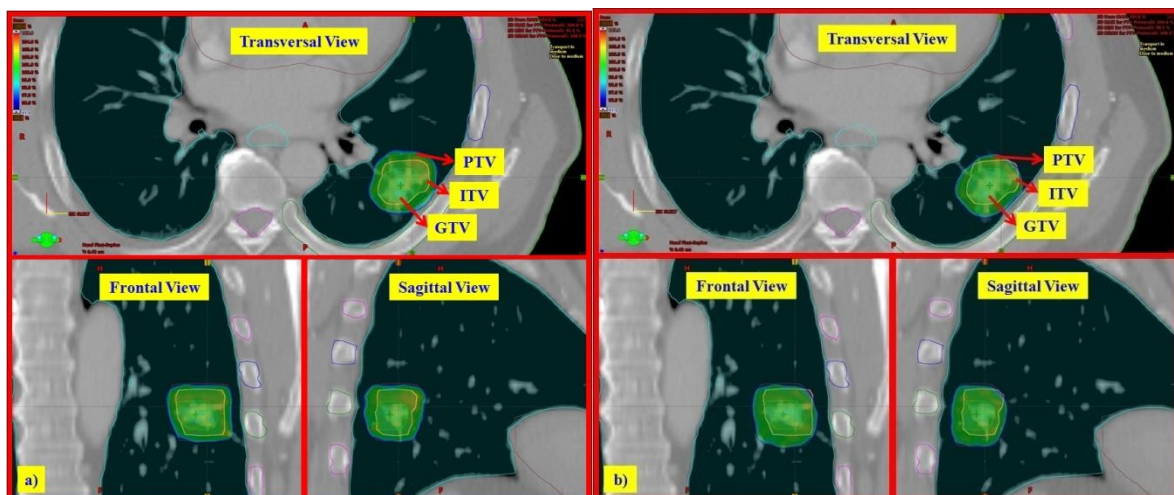


Figure 2. Variation of dose distribution in ITV due to strategies for PTV delineation (a) proposed strategy to delineate from ITV using multiple-phase 3D-CT (b) standard strategy to delineate from GTV using single

Table 4. Summary of tumor control probability for treatment volumes in peripherally and centrally located lesions

Treatment Volumes	End Stage		Breathing Phase	Peripheral		P-value	Central		P-value
				Proposed Plan	Standard Plan		Proposed Plan	Standard Plan	
ITV	36-Month Control	Local	RB	95.79±0.09	95.61±0.13	0.007	95.77±0.06	95.76±0.06	0.589
	Long Term Control	Local	RB	92.52±0.15	92.24±0.21	0.005	92.50±0.10	92.48±0.09	0.506
GTV	36-Month Control	Local	RB	95.77±0.12	95.70±0.12	0.193	95.77±0.06	95.76±0.06	0.589
			DIBH	96.21±0.55	96.05±0.48	0.016	95.78±0.06	95.77±0.06	0.655
			DEBH	96.09±0.25	95.97±0.20	0.203	95.77±0.06	95.76±0.05	0.546
			Combined	96.02±0.40	95.91±0.34	0.003	95.77±0.06	95.76±0.06	0.291
	Long Term Control	Local	RB	92.49±0.20	92.37±0.19	0.187	92.50±0.10	92.48±0.09	0.506
			DIBH	93.24±0.92	92.97±0.80	0.017	92.50±0.09	92.48±0.10	0.560
			DEBH	93.03±0.42	92.83±0.33	0.205	92.50±0.10	92.48±0.08	0.483
			Combined	92.92±0.67	92.72±0.57	0.003	92.50±0.10	92.48±0.09	0.193
ITV'	36-Month Control	Local	RB	95.79±0.10	95.61±0.14	< 0.001	95.76±0.08	95.75±0.06	0.071
	Long Term Control	Local	RB	92.52±0.17	92.24±0.23	< 0.001	92.49±0.13	92.46±0.11	0.012

ITV: tumor control probability calculated for internal target volume in RB phase, GTV: tumor control probability calculated for gross tumor volume during RB, DIBH, and DEBH breathing phases Combined - Mean value of RB, DIBH, and DEBH, ITV': tumor control probability calculated for internal treatment volume in RB phase with respect to post-treatment set-up variation of patients. RB: shallow breathing random phase, DIBH: deep inspiration breath-hold, DEBH: deep expiration breath-hold. TCP values are represented in percentage.

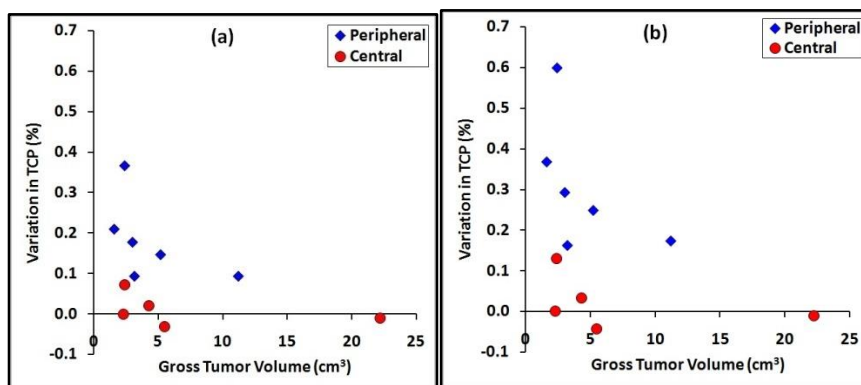


Figure3. Variation in TCP on the proposed plans with respect to standard plans for (a) 36-month local control and (b) long-term local control in peripherally and centrally located lung lesions.

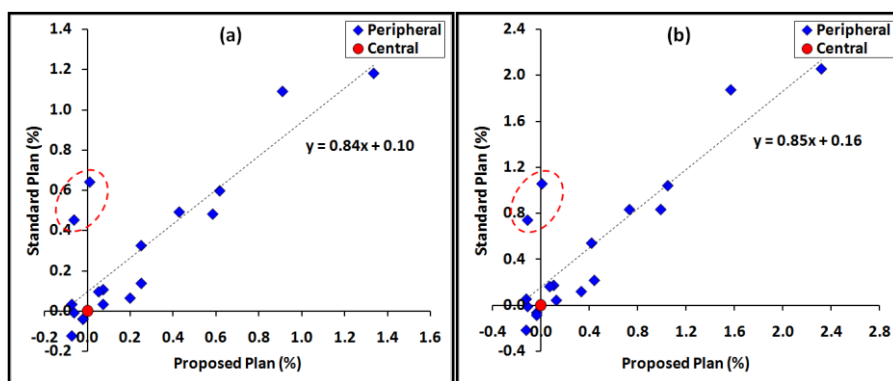


Figure4. Variation in TCP due to respiratory movements on the proposed plans and corresponding standard plans for (a) 36-month local control and (b) long-term local control in peripherally and centrally located lung lesion

Thirty-Six Month Local Control

Proposed and standard plans yielded TCP (36-month local control) of $95.79 \pm 0.09\%$ and $95.61 \pm 0.13\%$, respectively, with identical mean doses delivered to ITV in peripherally located lung lesions (Table4). In centrally located lung lesions, TCP of $95.77 \pm 0.06\%$ and $95.76 \pm 0.06\%$ were yielded by PP and SP, respectively.

Variations in TCP (ITV) between PP and SP were displayed with respect to tumor size and location in Figure 3 (a). As the ITV was encompassed by the proposed PTV, PP enhanced the TCP significantly up to 0.35% in peripherally located lung lesions ($P < 0.05$). However, in centrally located lung lesions, the difference in TCP between PP and SP was insignificant.

Table5. Summary of Normal Tissue Complication Probability for critical organs in peripherally and centrally located lesions

Organs	End Stage	Peripheral		P-value (n)	Central		P-value (n)
		Proposed Plan	Standard Plan		Proposed Plan	Standard Plan	
Lung	Pneumonitis, Grade \geq II	0.87 \pm 0.29	1.00 \pm 0.25	0.001 (6)	0.67 \pm 0.26	0.96 \pm 0.51	0.079 (5)
Rib	Pathologic fracture	29.50 \pm 27.20	36.98 \pm 32.64	0.064 (7)	25.28 \pm 18.3 7	36.47 \pm 26.83	0.117 (4)
Esophagus	Esophagitis, Grade \geq II	0.24 \pm 0.08	0.25 \pm 0.10	0.402 (5)	1.10 \pm 0.88	2.40 \pm 2.30	0.142 (5)
Trachea	Cartilage necrosis	0.00 \pm 0.00	0.00 \pm 0.00	-- (6)	26.74 \pm 1.99	61.30 \pm 11.33	-- (2)
Spinal Cord	Necrotic Myelitis	0.00 \pm 0.00	0.00 \pm 0.00	-- (6)	7.82 \pm 0.00	26.76 \pm 0.00	-- (1)
Heart	Pericarditis	0.00 \pm 0.00	0.00 \pm 0.00	-- (6)	0.00 \pm 0.00	0.00 \pm 0.00	-- (5)

NTCP values are represented in percentage. n: the sample size, (n-1): degree of freedom

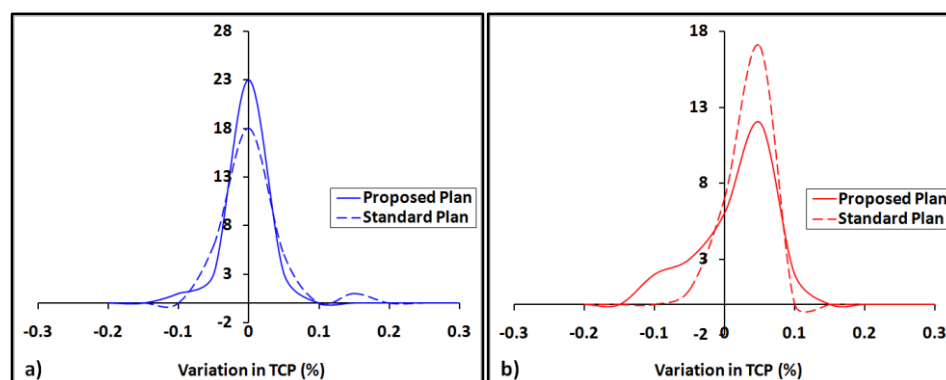


Figure5. Distribution of variation in TCP due to post-treatment set-up variations of patients between proposed and standard plans for a 36-month local control in (a) peripherally located and (b) centrally located lung lesions.

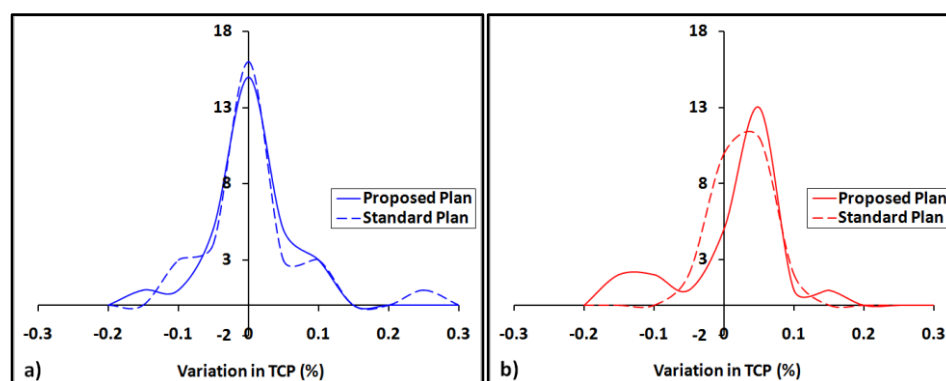


Figure6. Distribution of variation in TCP due to post-treatment set-up variations of patients between proposed and standard plans for long-term local control in (a) peripherally located and (b) centrally located lung lesions.

Long Term (> Five years) Local Control

In peripherally located lung lesions, TCP (Long term local control) remained at 92.52 \pm 0.15% and 92.24 \pm 0.21% for PP and SP, respectively (Table4). In centrally located lung lesions, TCP was 92.50 \pm 0.10% and 92.48 \pm 0.09% for PP and SP, respectively. Likewise, in 36-month local control, PP significantly enhanced the TCP for long term local control (0.6%) in peripherally located lung lesions, whereas the difference in TCP between PP and SP was insignificant in centrally located lesions, (Figure 3[b]).

Multiple Phase 3D-Dose Calculation

The multicenter trial urges that the GTV should be confined within PTV at any instance [15]. Accordingly, TCP was calculated through dose distribution in GTVs at DIBH, RB, and DEBH phases from PP and SP. The TCP varied based on the movement of GTV during respiratory motion due to the heterogeneous density of lung and tumor tissues (Table4). Compared to TCP of ITV, the TCP of GTV was enhanced in all the phases of respiratory motions during the treatment of peripherally located lesions (Figure 4). Meanwhile, in centrally located lung lesions, the negligible movement of GTV during respiratory motion led to an insignificant

difference between TCP of GTV and ITV. The TCPs were enhanced up to 1.2% and 2.0% during the respiratory motion for 36-month and long-term local control, respectively.

Normal Tissue Complication Probability

Normal tissue complication probabilities were calculated for different critical organs with specific endpoint/stage (Table5). In peripherally located lung lesions, NTCP were significantly low for the lungs; however, this level was not significantly low for other organs (rib and esophagus) with PP than the SP ($P < 0.05$). However, NTCPs remained null for the trachea, spinal cord, and heart in both plans. In centrally located lung lesions, there were significantly lower levels in PP with regard to NTCPs for all the critical organs. However, NTCPs were higher with SP and up to 35% for cartilage necrosis in the trachea and 19% for myelitis in the spinal cord.

Clinical Outcome

The obtained results of the current study revealed that 7 patients of this study had 11 lung lesions, out of which 6 were peripherally located and 5 were centrally located. The post-treatment clinical follow-ups of the patients who underwent SBRT-Lung were conducted after 6 and 12 months after treatment. The 12-month follow-ups revealed no residual tumors in the treatment beds of any patient as per the RECIST. A patient treated for a peripheral lung lesion reported that he experienced asymptomatic lung pneumonitis (ALP) in the dose fall-off region during his 6-month follow-up. However, his ALP decreased extensively over the next six months.

Discussion

The analysis of radiobiological parameters of TCP and NTCP revealed the significance of IMs in SBRT-Lung in the context of clinical utility. In this study, the IMs that accounted for tumor dislocations due to respiratory motions were derived using multiple-phase 3D-CT. In a clinical case study, the radiobiological utility of our institutional SBRT-lung protocol had a better performance with respect to several aspects than the multicenter trials based on 3D-CT [32].

The enhancement of toxicity to normal tissue due to the negligence of internal margins in SBRT-lung was discussed earlier [40, 41]. The IM estimations that were derived using multiphase 3D-CT or 4D-CT rendered a 50% reduction of PTV [17, 42-44] than conventional estimates [3]. In the current study, the ITV was identical to the GTV in centrally located lung lesions (Table3), leading to a 57% reduction of PTV than PTVs that were delineated using 3D-CT in multicenter trials [3, 15].

Furthermore, in the current study, the reduction in PTV levels results in the decrease of NTCP for the trachea from 61.30% of the standard plans to 26.74%. Correspondingly, the NTCP for the spinal cord was reduced to 7.82% from the standard plan value of 26.76% (Table5). Similarly, the NTCP for Grades \geq II

lung pneumonitis was significantly reduced in SBRT for peripherally located lung lesions because IMs were accounted for the delineated PTV. Excessive toxicities were predicted in our radiobiological analysis due to the omission of internal margins of standard PTV in the centrally located lesions. The current results were in agreement with the earlier observations of clinically excessive toxicities [40, 41, 45]. Excessive toxicities have been related to the biologically effective dose (BED) (their trial ≥ 180 Gy) [45], although the negligence of IMs was indeed a prognostic factor for NTCP and excessive toxicities.

In this study, the BED was 100 Gy (50 Gy in 5 fractions), which yielded TCP of ~95% and 92% for 36-month and long term local control, respectively. The BED of 100 Gy has been widely acknowledged to be sufficient for long-term local control [35, 46-49]. Guckenberger observed that the TCP was ~90% for a BED of 100 Gy with 4D-dose calculations, whereas the BED was 80 Gy with 3D-dose calculations [35]. Typical 4D-dose calculations indicated variations in absorbed dose due to MLC interplay effects, tumor dislocation during respiratory movements, and patient set-up variations during treatment.

Variations in prescribed dose delivery due to MLC interplay effects have been found to be negligible in SBRTs [50-54], particularly in SBRT-lung [51]. Therefore, the interplay effect was not emphasized in this report. The study was a thorough investigation of variations in dose distribution and the resultant TCPs due to tumor dislocation during respiratory movements and patient set-up variations during treatment. The variation in the TCP (GTV) was calculated as a surrogate for tumor dislocation during respiratory movements. When the TCP (GTV) was calculated at DIBH and DEBH phases, the volume of lung tissues in ITV was replaced by a relatively high-density GTV, and application of the Acuros algorithm increased the dose to GTV. As a result, the TCP (GTV) was enhanced during respiratory movements, compared to the TCP (ITV) on baseline CT dataset. The TCP (GTV) enhancement was proportionate in the both PTV delineation strategies, except when the ITV extended beyond the standard PTV (encircled in Figure 4). As ITV was identical to GTV in centrally located lung lesions, the TCP (GTV and ITV) remained unaltered during respiratory movements.

Variations in the TCP (ITV) with respect to patient set-up variations during treatment were retrospectively computed according to the patient data. The TCPs were remained consistent within $\pm 0.3\%$ both in proposed and standard plans (figure 5 and 6). The PTV generated with a 3-mm margin from ITV on 4D-CT rendered good local control with lesser toxicities [42, 43, 55]. Similarly, in the current study, a 3-mm PTV margin from the ITV reduced the NTCP and improved the TCP. Consequently, an optimum therapeutic ratio was obtained by the proposed PTV margin in SBRT-Lung with 3D-CT acquired at multiple phases of respiratory movements.

Conclusion

During SBRT-Lung, the reproducible positioning of the tumor that is computed on the basis of baseline CT datasets remains vital in delineating the treatment volume. This is more likely to be achieved with tumor motion mitigation accessories. The estimation of IM in PTV assured the reliability of delineated treatment volume and reduced complications due to the irradiation of surrounding normal tissues. The PTV margin derived from ITV, reduced the NTCP both in centrally and peripherally located lung lesions; however, it enhanced TCP in peripherally located lung lesions for the given BED (100 Gy). The current study demonstrates that the strategy of delineating treatment volume using multiple-phase 3D-CT has the potential to reduce complications in irradiated normal tissues and enhance therapeutic gains in SBRT-Lung. The proposed strategy has the potential to yield comparable lesser toxicities as in 4D-CT strategy.

Acknowledgment

The authors are grateful to the Head of Jaypee Hospital, Noida, India for constantly supporting our academic and research pursuits. We are especially thankful to Dr. Sudarsan De, Director-Cancer Care and the team of radiotherapists of the hospital where the work was carried out.

References

- Xia T, Li H, Sun Q, Wang Y, Fan N, Yu Y, et al. Promising clinical outcome of stereotactic body radiation therapy for patients with inoperable Stage I/II non-small-cell lung cancer. *Int J Radiat Oncol Biol Phys.* 2006 Sep 1;66(1):117-25.
- Baumann P, Nyman J, Hoyer M, Wennberg B, Gagliardi G, Lax I, et al. Outcome in a prospective phase II trial of medically inoperable stage I non small-cell lung cancer patients treated with stereotactic body radiotherapy. *J Clin Oncol.* 2009 Jul 10;27(20):3290-6.
- Timmerman R, Paulus R, Galvin J, Michalski J, Straube W, Bradley J, et al. Stereotactic body radiation therapy for inoperable early stage lung cancer. *JAMA.* 2010 Mar 17;303(11):1070-6.
- Chang JY, Senan S, Paul MA, Mehran RJ, Louie AV, Balter P, et al. Stereotactic ablative radiotherapy versus lobectomy for operable stage I non-small-cell lung cancer: a pooled analysis of two randomised trials. *Lancet Oncol.* 2015 Jun;16(6):630-7.
- Soldà F, Lodge M, Ashley S, Whittington A, Goldstraw P, Brada M. Stereotactic radiotherapy (SABR) for the treatment of primary non-small cell lung cancer; systematic review and comparison with a surgical cohort. *Radiother Oncol.* 2013 Oct;109(1):1-7.
- Zheng X, Schipper M, Kidwell K, Lin J, Reddy R, Ren Y, et al. Survival outcome after stereotactic body radiation therapy and surgery for stage I non-small cell lung cancer: a meta-analysis. *Int J Radiat Oncol Biol Phys.* 2014 Nov 1;90(3):603-11.
- Zhang B, Zhu F, Ma X, Tian Y, Cao D, Luo S, et al. Matched-pair comparisons of stereotactic body radiotherapy (SBRT) versus surgery for the treatment of early stage non-small cell lung cancer: a systematic review and meta-analysis. *Radiother Oncol.* 2014 Aug;112(2):250-5.
- ICRU Report 62. International Commission on Radiation Units and Measurements. Prescribing, Recording, and Reporting Photon Beam Therapy, Supplement to ICRU Report No. 50. Bethesda, MD: ICRU;1999.
- Shimizu S, Shirato H, Ogura S, Akita-Dosaka H, Kitamura K, Nishioka T, et al. Detection of lung tumor movement in real-time tumor-tracking radiotherapy. *Int J Radiat Oncol Biol Phys.* 2001 Oct 1;51(2):304-10.
- Chen QS, Weinhaus MS, Deibel FC, Ciezki JP, Macklis RM. Fluoroscopic study of tumor motion due to breathing: Facilitating precise radiation therapy for lung cancer patients. *Med Phys.* 2001 Sep;28(9):1850-6.
- Sixel KE, Ruschin M, Tirone R, Cheung PC. Digital fluoroscopy to quantify lung tumor motion: Potential for patient-specific planning target volumes. *Int J Radiat Oncol Biol Phys.* 2003 Nov 1;57(3):717-23.
- Yu ZH, Lin SH, Balter P, Zhang L, Dong L. A comparison of tumor motion characteristics between early stage and locally advanced stage lung cancers. *Radiother Oncol.* 2012 Jul;104(1):33-8.
- Plathow C, Ley S, Fink C, Puderbach M, Hosch W, Schmähl A, et al. Analysis of intrathoracic tumor mobility during whole breathing cycle by dynamic MRI. *Int J Radiat Oncol Biol Phys.* 2004 Jul 15;59(4):952-9.
- Erridge SC, Seppenwoolde Y, Muller SH, van Herk M, De Jaeger K, Belderbos JS, et al. Portal imaging to assess set-up errors, tumor motion and tumor shrinkage during conformal radiotherapy of non-small cell lung cancer. *Radiother Oncol.* 2003 Jan;66(1):75-85.
- Videtic GM, Hu C, Singh AK, Chang JY, Parker W, Olivier KR, et al. A Randomized Phase 2 Study Comparing 2 Stereotactic Body Radiation Therapy Schedules for Medically Inoperable Patients with Stage I Peripheral Non-Small Cell Lung Cancer: NRG Oncology RTOG 0915 (NCCTG N0927). *Int J Radiat Oncol Biol Phys.* 2015 Nov 15;93(4):757-64.
- Wang L, Hayes S, Paskalev K, Jin L, Buyyounouski MK, Ma CC, et al. Dosimetric comparison of stereotactic body radiotherapy using 4D CT and multiphase CT images for treatment planning of lung cancer: evaluation of the impact on daily dose coverage. *Radiother Oncol.* 2009 Jun;91(3):314-24.
- Underberg RW, Lagerwaard FJ, Cuijpers JP, Slotman BJ, van Sörnsen de Koste JR, Senan S. 4-dimensional CT scans for treatment planning in stereotactic radiotherapy for Stage I lung cancer. *Int J Radiat Oncol Biol Phys.* 2004 Nov 15;60(4):1283-90.
- Lagerwaard FJ, Van Sörnsen de Koste JR, Nijssen-Visser MR, Schuchhard-Schipper RH, Oei SS, Munne A, et al. Multiple "slow" CT scans for incorporating lung tumor mobility in radiotherapy planning. *Int J Radiat Oncol Biol Phys.* 2001 Nov 15;51(4):932-7.

19. Wurstbauer K, Deutschmann H, Kopp P, Sedlmayer F. Radiotherapy planning for lung cancer: Slow CTs allow the drawing of tighter margins. *Radiother Oncol.* 2005 May;75(2):165-70.
20. Shih HA, Jiang SB, Aljarrah KM, Doppke KP, Choi NC. Internal target volume determined with expansion margins beyond composite gross tumor volume in three-dimensional conformal radiotherapy for lung cancer. *Int J Radiat Oncol Biol Phys.* 2004 Oct 1;60(2):613-22.
21. Therasse P, Arbuck SG, Eisenhauer EA, Wanders J, Kaplan RS, Rubinstein L, et al. New guidelines to evaluate the response to treatment in solid tumors. *J Natl Cancer Inst.* 2000 Feb 2;92(3):205-16.
22. Ohri N, Werner-Wasik M, Grills IS, Belderbos J, Hope A, Yan D, et al. Modeling local control after hypofractionated stereotactic body radiation therapy for stage I non-small cell lung cancer: a report from the elekta collaborative lung research group. *Int J Radiat Oncol Biol Phys.* 2012 Nov 1;84(3):379-84.
23. Gay HA, Niemierko A. A free program for calculating EUD-based NTCP and TCP in external beam radiotherapy. *Phys Med.* 2007 Dec;23(3-4):115-25.
24. Martel MK, Ten Haken RK, Hazuka MB, Kessler ML, Strawderman M, Turrisi AT, et al. Estimation of tumor control probability model parameters from 3-D dose distributions of non-small cell lung cancer patients. *Lung Cancer.* 1999 Apr;24(1):31-7.
25. Fenwick JD, Nahum AE, Malik ZI, Eswar CV, Hatton MQ, Laurence VM, et al. Escalation and intensification of radiotherapy for stage III non-small cell lung cancer: opportunities for treatment improvement. *Clin Oncol (R Coll Radiol).* 2009 May;21(4):343-60.
26. Webb S, Nahum AE. A model for calculating tumour control probability in radiotherapy including the effects of inhomogeneous distributions of dose and clonogenic cell density. *Phys Med Biol.* 1993 Jun;38(6):653-66.
27. Huang BT, Lu JY, Lin PX, Chen JZ, Li DR, Chen CZ. Radiobiological modeling analysis of the optimal fraction scheme in patients with peripheral non-small cell lung cancer undergoing stereotactic body radiotherapy. *Sci Rep.* 2015 Dec 11;5:18010.
28. Kim MS, Kim W, Park IH, Kim HJ, Lee E, Jung JH, et al. Radiobiological mechanisms of stereotactic body radiation therapy and stereotactic radiation surgery. *Radiat Oncol J.* 2015 Dec; 33(4): 265-75.
29. Ruggieri R, Stavrev P, Naccarato S, Stavreva N, Alongi F, Nahum AE. Optimal dose and fraction number in SBRT of lung tumours: A radiobiological analysis. *Phys Med.* 2017 Dec;44:188-95.
30. Brenner DJ. The linear-quadratic model is an appropriate methodology for determining isoeffective doses at large doses per fraction. *Semin Radiat Oncol.* 2008 Oct;18(4):234-9.
31. Lovelock DM, Zatzky J, Goodman K, Yamada Y. The Effectiveness of a Pneumatic Compression Belt in Reducing Respiratory Motion of Abdominal Tumors in Patients Undergoing Stereotactic Body Radiotherapy. *Technol Cancer Res Treat.* 2014 Jun;13(3):259-67.
32. Chairmadurai A, Goel HC, Jain SK, Kumar P. Radiobiological analysis of stereotactic body radiation therapy for an evidence-based planning target volume of the lung using multiphase CT images obtained with a pneumatic abdominal compression apparatus: a case study. *Radiol Phys Technol.* 2017 Dec;10(4):525-34.
33. Purdie TG, Bissonnette JP, Franks K, Bezjak A, Payne D, Sie F, et al. Cone-beam computed tomography for on-line image guidance of lung stereotactic radiotherapy: localization, verification, and intrafraction tumor position. *Int J Radiat Oncol Biol Phys.* 2007 May 1;68(1):243-52.
34. Bissonnette JP, Franks KN, Purdie TG, Moseley DJ, Sonke JJ, Jaffray DA, et al. Quantifying interfraction and intrafraction tumor motion in lung stereotactic body radiotherapy using respiration-correlated cone beam computed tomography. *Int J Radiat Oncol Biol Phys.* 2009 Nov 1;75(3):688-95.
35. Guckenberger M, Wulf J, Mueller G, Krieger T, Baier K, Gabor M, et al. Dose-response relationship for image-guided stereotactic body radiotherapy of pulmonary tumors: relevance of 4D dose calculation. *Int J Radiat Oncol Biol Phys.* 2009 May 1;74(1):47-54.
36. Muller-Runkel R, Vijayakumar S. Equivalent total doses for different fractionation schemes, based on the linear quadratic model. *Radiology.* 1991 May;179(2):573-7.
37. AgrenCronqvist AK, Källman P, Turesson I, Brahme A. Volume and heterogeneity dependence of the dose-response relationship for head and neck tumours. *Acta Oncol.* 1995;34(6):851-60.
38. Seppenwoolde Y, Lebesque JV, de Jaeger K, Belderbos JS, Boersma LJ, Schilstra C, et al. Comparing different NTCP models that predict the incidence of radiation pneumonitis. Normal tissue complication probability. *Int J Radiat Oncol Biol Phys.* 2003 Mar 1;55(3):724-35.
39. Chapet O, Kong FM, Lee JS, Hayman JA, Ten Haken RK. Normal tissue complication probability modeling for acute esophagitis in patients treated with conformal radiation therapy for non-small cell lung cancer. *Radiother Oncol.* 2005 Nov;77(2):176-81.
40. Senan S, Haasbeek NJ, Smit EF, Lagerwaard FJ. Stereotactic radiotherapy for centrally located early-stage lung tumors. *J Clin Oncol.* 2007 Feb 1;25(4):464.
41. Onimaru R, Shirato H, Shimizu S, Kitamura K, Xu B, Fukumoto S, et al. Tolerance of organs at risk in small-volume, hypofractionated, image-guided radiotherapy for primary and metastatic lung cancers. *Int J Radiat Oncol Biol Phys.* 2003 May 1;56(1):126-35.
42. Hurkmans CW, Cuijpers JP, Lagerwaard FJ, Widder J, van der Heide UA, Schuring D, et al. Recommendations for implementing stereotactic radiotherapy in peripheral stage IA non-small cell lung cancer: report from the Quality Assurance Working Party of the randomised phase III ROSEL study. *Radiat Oncol.* 2009 Jan 12;4:1.
43. Lagerwaard FJ, Haasbeek CJ, Smit EF, Slotman BJ, Senan S. Outcomes of risk-adapted fractionated stereotactic radiotherapy for stage I non-small-cell lung cancer. *Int J Radiat Oncol Biol Phys.* 2008 Mar 1;70(3):685-92.
44. Haasbeek CJ, Senan S, Smit EF, Paul MA, Slotman BJ, Lagerwaard FJ. Critical review of nonsurgical treatment options for stage I non-small cell lung cancer. *Oncologist.* 2008;13:309-19.

45. Timmerman R, McGarry R, Yiannoutsos C, Papiez L, Tudor K, DeLuca J, et al. Excessive toxicity when treating central tumors in a phase II study of stereotactic body radiation therapy for medically inoperable early-stage lung cancer. *J Clin Oncol*. 2006 Oct 20;24(30):4833-9.
46. Lagerwaard FJ, van der Geld Y, Slotman BJ, Senan S. Quality of life after stereotactic radiotherapy for medically inoperable stage I non-small cell lung cancer. *Int J Radiat Oncol Biol Phys*. 2006 Nov 1;66(1):S133-S4.
47. Fowler JF, Tomé WA, Fenwick JD, Mehta MP. A challenge to traditional radiation oncology. *Int J Radiat Oncol Biol Phys*. 2004 Nov 15;60(4):1241-56.
48. Onishi H, Araki T, Shirato H, Nagata Y, Hiraoka M, Gomi K, et al. Stereotactic hypofractionated high-dose irradiation for stage I non-small cell lung carcinoma: Clinical outcomes in 245 subjects in a Japanese multi institutional study. *Cancer*. 2004 Oct 1;101(7):1623-31.
49. Wulf J, Baier K, Mueller G, Flentje MP. Dose-response in stereotactic irradiation of lung tumors. *Radiother Oncol*. 2005 Oct;77(1):83-7.
50. Yoganathan SA, Maria Das KJ, Agarwal A, Kumar S. Magnitude, Impact, and Management of Respiration-induced Target Motion in Radiotherapy Treatment: A Comprehensive Review. *J Med Phys*. 2017 Jul-Sep;42(3):101-15.
51. Li X, Yang Y, Li T, Fallon K, Heron DE, Huq MS. Dosimetric effect of respiratory motion on volumetric-modulated arc therapy-based lung SBRT treatment delivered by trueBeam machine with flattening filter-free beam. *J Appl Clin Med Phys*. 2013 Nov 4;14(6):4370.
52. Ong C, Verbakel WF, Cuijpers JP, Slotman BJ, Senan S. Dosimetric impact of interplay effect on rapidArc lung stereotactic treatment delivery. *Int J Radiat Oncol Biol Phys*. 2011 Jan 1;79(1):305-11.
53. Stambaugh C, Nelms BE, Dilling T, Stevens C, Latifi K, Zhang G, et al. Experimentally studied dynamic dose interplay does not meaningfully affect target dose in VMAT SBRT lung treatments. *Med Phys*. 2013 Sep;40(9):091710.
54. Rao M, Wu J, Cao D, Wong T, Mehta V, Shepard D, et al. Dosimetric impact of breathing motion in lung stereotactic body radiotherapy treatment using intensity modulated radiotherapy and volumetric modulated arc therapy [corrected]. *Int J Radiat Oncol Biol Phys*. 2012 Jun 1;83(2):e251-6.
55. Schuring D, Hurkmans CW. Developing and evaluating stereotactic lung RT trials: what we should know about the influence of inhomogeneity corrections on dose. *Radiat Oncol*. 2008 Jul 28;3:21.